System identification of a large scale swirled premixed combustor using LES and comparison to measurements.

Giauque A.[1], Selle L.[1], Poinsot T.[2], Buechner H.[3], Kaufmann P.[4] and Krebs W.[4]

November 28, 2003

[1]CERFACS
31057 TOULOUSE CEDEX FRANCE

[2]Institut de Mécanique des Fluides de Toulouse
31400 TOULOUSE FRANCE

[3]Engler Bunte Institute, Karlsruhe University
Karlsruhe GERMANY

[4]Siemens PG
45466 Mullheim GERMANY

Corresponding author:
Alexis GIAUQUE
CERFACS
42 Avenue Coriolis
31057 TOULOUSE CEDEX FRANCE
FAX: 33 5 61 19 30 00
EMAIL: giauque@cerfacs.fr

Colloqium:
Propulsion and engines combustion

Short title:
LES and measurements of forced swirled flame.

Total length of paper:
5830 words.

List of the word equivalent lengths:

Main text	2000 words	References	510 words	Figure 1	118 words
Figure 2	131 words	Figure 3	420 words	Figure 4	391 words
Figure 5	140 words	Figure 6	174 words	Figure 7	126 words
Figure 8	672 words	Figure 9	175 words	Figure 10	276 words
Figure 11	146 words	Figure 12	210 words	Figure 13	142 words
Equations	100 words				

Abstract

The forced response of a swirled premixed burner to acoustic excitations is computed with Large Eddy Simulation and compared to measurements performed at University of Karlsruhe. The configuration is a 1:1 representation of a prototype industrial burner provided by Siemens in which gases are injected through two complex-geometry swirlers. Thanks to hybrid meshes and parallel computations, the simulation integrates a large part of this complex geometry. The inlet of the largest swirler is forced with acoustic waves at frequencies varying from 80 to 250 Hz and the LES data is compared to experimental results in terms of combustion delay. The LES also gives access to the forced flow topology, revealing that the excitation creates large toroidal vortices which distort the flame surface and destabilize downstream of the burner mouth. In addition to these toroidal vortices, LES also reveals that a precessing vortex core appears when excitation is started.

Keywords:
GAS TURBINES, ACOUSTICS, LARGE EDDY SIMULATION

1 Introduction

Being able to predict the forced response of a combustion device is one mandatory step to design 'stable' burners, ie burners which exhibit as little sensitivity to acoustic waves as possible. Indeed, flame acoustic coupling is a phenomenon which is found in multiple combustors[1, 2, 3, 4, 5, 6, 7]: it creates a considerable industrial risk if it cannot be avoided at the design stage. However, predicting flame / acoustics coupling is still a challenge [4, 5]. Few comparisons including experiments and simulations can be found in the literature on flame transfer function in complex configurations. This study shows how experiments and Large Eddy Simulations (LES) can be used in realistic geometries to provide one essential element to predict flame stability: the flame response to acoustic waves entering the burner. This response is characterized through the transfer function between unsteady heat release in the chamber and oscillating inlet velocity. The experimental configuration is described first. The LES tools and the methodology used to introduce acoustic waves through boundaries are then presented before describing results.

2 A double swirler premixed burner

The burner used for this study is a modified version of a Siemens hybrid burner used here at atmospheric pressure (maximum power = 400 kW). The burner (Fig. 1) is mounted on a cylindrical combustion chamber (Fig. 2). The configuration used for experiments is described on Fig. 3. Fully premixed methane / air is injected through two coaxial swirlers (diagonal and axial) at an equivalence ratio of 0.8 for the axial and 0.5 for the diagonal swirler. The pulsating unit is a rotating valve modulating the diagonal mass flow rate up to amplitudes of 30 percent. The unsteady velocity induced by forcing is measured using a hot wire probe located in the diagonal swirler (Fig. 1) while the global unsteady heat release is evaluated through a measurement of the OH* radical. Since 90% of the injected mixture is at a constant equivalence ratio, the OH* signal can be reliably linked to the unsteady heat release [6]. Figure 4 displays typical flame shapes observed without forcing or with low frequency forcing (left) and with high-frequency forcing (right). The flame is quasi-steady as long as the frequency of the excitation remains below 50Hz. Beyond this limit, ring vortices interact with the flame imposing their axi-symmetrical shape to the flame.

3 Large Eddy Simulations for gas turbines

Recent studies [8, 9, 10, 11, 12] have shown that Large Eddy Simulations (LES) are powerful tools to study the dynamics of turbulent flames and especially their response to acoustic forcing. However, the extension of LES methods to complex geometries creates new problems to adapt high-precision numerical techniques (required for LES) to arbitrarily complex meshes. Here a parallel LES solver called AVBP (see www.cerfacs.fr/cfd/) is used to solve the full compressible Navier Stokes equations on hybrid (structured and unstructured) grids with third-order spatial and temporal accuracy [13]. Subgrid stresses are described by the WALE model [14]. The subgrid flame / turbulence interaction is modeled by the Thickened Flame (TF) model [8, 13]. For the present application, methane / air combustion is modelled using six species (CH_4,O_2, CO_2, CO, H_2O and N_2) and two reactions [15]. These reactions are :

$$CH_4 + 3/2O_2 => CO + 2H_2O \tag{1}$$

$$CO + 1/2O_2 <=> CO_2 \tag{2}$$

The forward rate of the first irreversible reaction is:

$$q_1 = AY_{CH_4}^{0.9}\, Y_{O_2}^{1.1}\, exp(-T_a^1/T)$$

and the rate of the second reaction is:

$$q_2 = B[Y_{CO}\, Y_{O_2}^{0.5} - (1/K_y)\, Y_{CO_2}]\, exp(-T_a^2/T)$$

where $A = 6.1.10^8\ mol.m^{-3}.s^{-1}$, $B = 6.1.10^5\ mol.m^{-3}.s^{-1}$, $T_a^1 = 17613$ K, $T_a^2 = 6038$ K and $K_y(T)$ is the equilibrium constant of the reaction (2). The mesh used for the burner of this study contains 1.7 million elements.

4 Introducing acoustic waves through the burner inlet

To determine the transfer function of a burner, the usual procedure is to introduce an acoustic wave into the burner and measure the perturbation of heat release. The time delay between the incoming unsteady flow rate and the unsteady heat release is an essential ingredient of acoustic approaches for combustor stability[4 , 16, 17, 18, 19, 20]. Experimentally, this is usually done with loudspeakers forcing the flow upstream or downstream of the combustion chamber. At high chamber powers, however, rotating valves are required as done here in Karlsruhe. Because of the cost of such devices and the danger of pulsating large flow rates of premixed gases, performing the same task with LES is an obvious alternative path. However, the exact numerical procedure to introduce acoustic waves in a computation is a difficult topic and may lead to numerical artefacts [21]. In a compressible LES, each boundary must be specified in terms of mean conditions (velocity or pressure for example) but also in terms of acoustic impedance. Many methods for such problems are based on characteristic methods [4, 22] but must be used with care: the well - known ‘non reflecting’ conditions actually impose an impedance (which is often unknown) and can have a strong influence on the results[23]. For a simple laminar flame, Kaufmann et al[24] show that a proper method to excite a combustion chamber is to pulsate the incoming acoustic wave and not the local velocity. This procedure is used here and avoids false numerical resonances when the chamber is forced.

5 Reacting steady flow

Since the focus of this paper is the forced response of the burner, no experimental results will be provided for the unforced case. The non-reacting and reacting flow for this burner installed in a slightly different combustion chamber have been computed in previous studies and successfully compared to experiments in terms of axial and tangential velocities (mean and RMS) and mean temperature fields[15,23]: this validation is not repeated here.

The reacting case corresponds to a global equivalence ratio of 0.51, air flow rate of 180 g/s, a Reynolds number of 1.210^5 (based on bulk velocity and burner diameter) and power of 277 kW. A 2D snapshot of the temperature field (Fig. 5) shows a compact flame located close to the burner mouth, stabilized both on the inner recirculation zone created by swirl and on the outer recirculation zones. A leaner and weaker flame front can be identified in front of the diagonal swirler inlet. A temperature isosurface at 1000 K (Fig. 6) shows the typical flame shape: the edges of the flame are oscillating but the central zone, near the axial inlet, is very stable.

6 Forced reacting flow

The experimental device was forced for frequencies changing from 10 to 120 Hz while the LES were performed at 80, 120 and 250 Hz. Figure 7 shows a longitudinal cut of the temperature field: the solid line delineates backflow regions where the axial velocity is negative. This flame is caracterised by two different behaviours. Near the axial burner a rich and thus warm flame is found. The diagonal swirler is injecting leaner gases and this flame is more affected by the excitation. This is confirmed by 3D snapshots of the flame which exhibit the presense of cusps and spherical structures of unburned gas in front of the diagonal swirler (Fig. 8 (d)).
The inlet forcing leads to the apparition of an heat release oscillation. Figure 9 compares evolutions of heat release, diagonal inlet velocity and total mass of fuel in the chamber for the 120Hz case. While the inlet velocity (circles) and the enclosed fuel mass (deltas) oscillate sinusoidally, the total heat release exhibits more nonlinearities, decreasing very rapidly between instants a) and b). Four phases of the cycle are presented (Fig. 8) ($\phi = 0$, $\pi/2$, π, $3\pi/2$). The phase $\phi = 0$ corresponds to the minimum value of the axial velocity whereas $\phi = \pi$ corresponds to the maximum value of the axial velocity. The flame surface varies through the cycle and exhibits various complex structures especially at $\phi = 3\pi/2$ (Fig. 8). The total heat release oscillates from 0.7 to 1.3 times its steady value (Fig. 9) at 180^o of the inlet velocity. The flame goes through phases of rapid expansion (between instants c and d on Fig 8 for example) during which ring vortices created by the forcing distort the flame front and expand it. Later in the cycle, the flame shrinks very fast (between instants a and b on fig 8) when the fresh gases injected previously burn out.

7 Coherent structures

LES reveals that two coherent structures determine the flame shape and the structure of the flow. Figure 10 displays the classical ring vortex structure observed in this configuration. The excitation creates a large axisymetrical ring which is convected by the mean flow and interacts with the flame, increasing the flame surface as it passes through. This ring is visualized here using a detection criterion based on the second invariant of the velocity tensor[25].
A second structure generated by the axial forcing is the precessing vortex core. This instability is typical of non reacting swirling flows [26] but was not observed for the unforced reacting case. Velocities and pressure at the point A displayed on Fig. 5 start to oscillate as soon as the flame is excited (after 25 ms on Fig. 11). A visualisation of the vortex criterion (Fig. 12) excluding the large vortex ring of Fig. 10 reveals a coherent structure rotating around the chamber axis. The frequency of this precessing structure is independant of the pulsation frequency and remains around 75 Hz.

8 Comparison of LES and experiment

Figure 13 compares numerical predictions and experimental measurements of the flame tranfer function using the n-tau model [4, 16]. This model links the heat release fluctuation $\dot{w}(t)$ to the velocity fluctuation at the inlet $u'(t)$ by :

$$ne^{iw\tau} = \frac{\gamma - 1}{S_D \gamma p_0} \frac{\int \dot{w}(t)\, dV}{u'(t)}$$

where p_0 is the mean pressure in the combustion chamber and S_D the diagonal swirler inlet surface of fuel injection. Values of the time delay τ (expressed here as a phase shift $\phi = -w\tau - 2\pi$) are in good agreement with experimental values (Fig. 13). The time lag between heat release and velocity fluctuations is of the order of $4.7ms$ and is mainly due to the convection time between swirler exit and flame front, confirming other CFD analysis [6, 7].

9 Conclusions

Large Eddy Simulation is used to compute the forced response of an acoustically excited swirled burner. The configuration is a 1:1 representation of a prototype gas turbine burner provided by Siemens in which premixed gases are injected through two complex-geometry swirlers. The LES solver uses hybrid meshes and high-order schemes. Combustion/turbulence interaction is modeled using the thickened flame model. A two-step scheme for methane/air combustion is used to represent chemistry. A comparison of combustion delays given by LES and measurements performed in Karlsruhe is made and the agreement between those is good. Exciting the main inlet at frequencies varying from 80 to 250 Hz, two main flow structures are evidenced by LES:

- A toroidal structure which modulates the global heat release by interacting with the flame surface.
- A precessing vortex core attached to the center of the axial swirler and whose frequency is independant of the inlet excitation frequency.

More generally, this study confirms the potential of LES to study turbulent combustion in complex geometries.

10 Acknowledgments

The support of Siemens is gratefully acknowledged.

11 References

1. Williams, F. A., *Combustion theory.* Benjamin Cummings, Menlo Park, CA, 1985.
2. Crighton, D. G., Dowling, A., Ffowcs Williams, J., Heckl, M. and Leppington, F., *Modern methods in analytical acoustics.* Springer Verlag, 1992.
3. Candel, S., Huynh, C. and Poinsot, T., in *Unsteady combustion* Nato ASI Series, Kluwer Academic Publishers, Dordrecht, 1996, p. 83-112.
4. Poinsot, T. and Veynante, D., *Theoretical and numerical combustion.* R.T. Edwards, 2001.
5. Krebs, W., Flohr, P., Prade, B. and Hoffmann, S., *Combustion Science and Technology* 174: 99-128 (2002).
6. Lohrmann, M., Buchner, H., Zarzalis, N. and Krebs, W., Atlanta, Georgia, USA, *ASME TURBO EXPO 2003,* ASME Paper 2003-GT-38114 (2003).
7. Buchner, H., Lohrmann, M., Krebs, W., Hoffmann, S. and Prade, B., Amsterdam, NL, *ASME TURBO EXPO 2002,* ASME Paper 2002-GT-30065 (2002).
8. Angelberger, C., Egolfopoulos, F. and Veynante, D., *Flow Turb. and Combustion* 65: 205-22 (2000).
9. Caraeni, D., Bergström, C. and Fuchs, L., *Flow Turb. and Combustion* 65: 223-244 (2000).
10. Colin, O. and Rudgyard, M., *J. Comput. Phys.* 162: 338-371 (2000).
11. Pitsch, H. and Duchamp de la Geneste, L., *Proc of the Comb. Institute* 29: 2001-2008 (2002).
12. Sankaran, V. and Menon, S., *J. of Turbulence* 3: 011 (2002).
13. Colin, O., Ducros, F., Veynante, D. and Poinsot, T., *Phys. Fluids* 12: 1843-1863 (2000).
14. Nicoud, F. and Ducros, F., *Flow Turb. and Combustion* 62: 183-200 (1999).
15. Selle, L., Lartigue, G., Poinsot, T., Kaufman, P., Krebs, W. and Veynante, D., in *Proc. of the Summer Program* Center for Turbulence Research, NASA Ames/Stanford Univ., 2002, p. 333-345.
16. Crocco, L., *12th Symp. (Int.) on Combustion,* 85-99, The Combustion Institute, Pittsburgh, (1969).
17. Hsiao, G., Pandalai, R., Hura, H. and Mongia, H., AIAA Paper 98-3380 (1998).
18. Krueger, U., Hueren, J., Hoffmann, S., Krebs, W., Flohr, P. and Bohn, D., *ASME TURBO EXPO 2000,* ASME Paper 2000-GT-0095 (2000).
19. Paschereit, C. O., Flohr, P. and Schuermans, B., Reno, NV, *39th AIAA Aerospace Sciences Meeting and Exhibit,* AIAA Paper 2001-0484 (2001).
20. Polifke, W., Poncet, A., Paschereit, C. O. and Doebbeling, K., *J. Sound Vibration* 245: 483-510 (2001).
21. Poinsot, T. and Lele, S., *J. Comput. Phys.* 101: 104-129 (1992).
22. Giles, M., *AIAA Journal* 28: 2050-2058 (1990).
23. Selle, L., "Large Eddy Simulation of flame/acoustic interaction in a swirled flow.," INP, (2003).

24. Kaufmann, A., Nicoud, F. and Poinsot, T., *Combust. Flame* 131: 371-385 (2002).

25. Hussain, F. and Jeong, J., *J. of Fluid Mech.* 285: 69-94 (1995).

26. Lucca-Negro, O. and O'Doherty, T., *Prog. Energy Comb. Sci.* 27: 431-481 (2001).

List of Figures

12 Figures

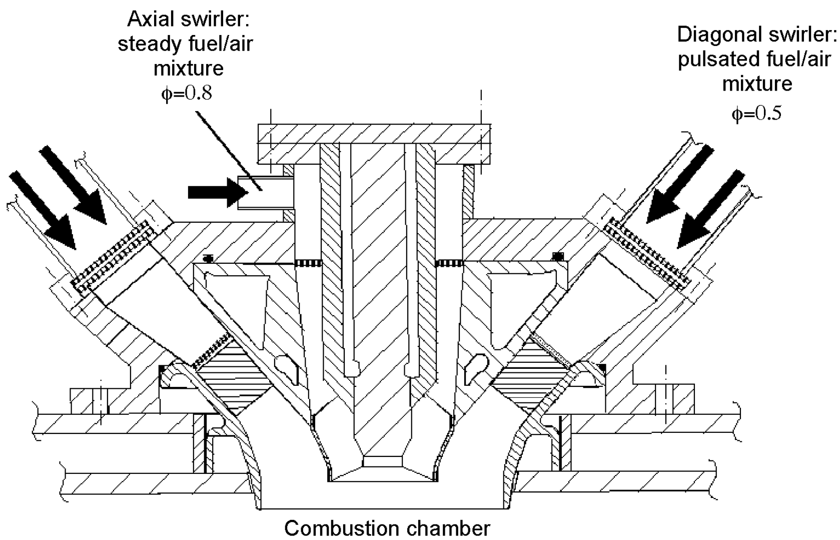

Figure 1: Burner configuration.

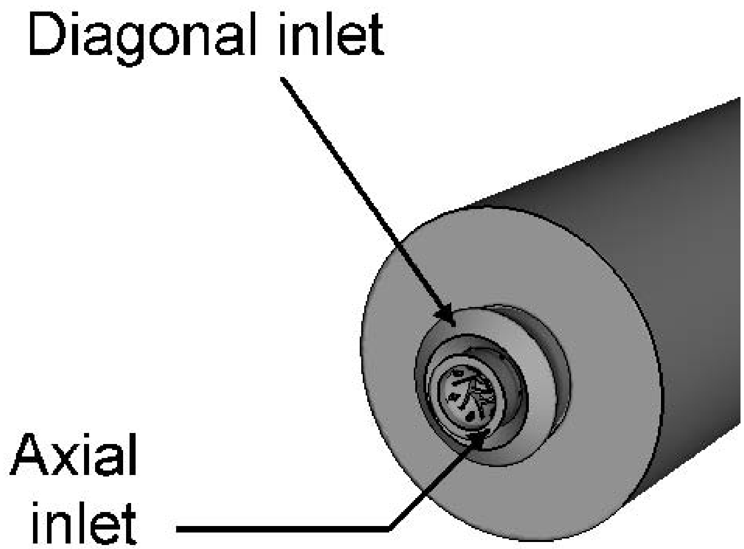

Figure 2: Burner mounted on EBI combustion chamber

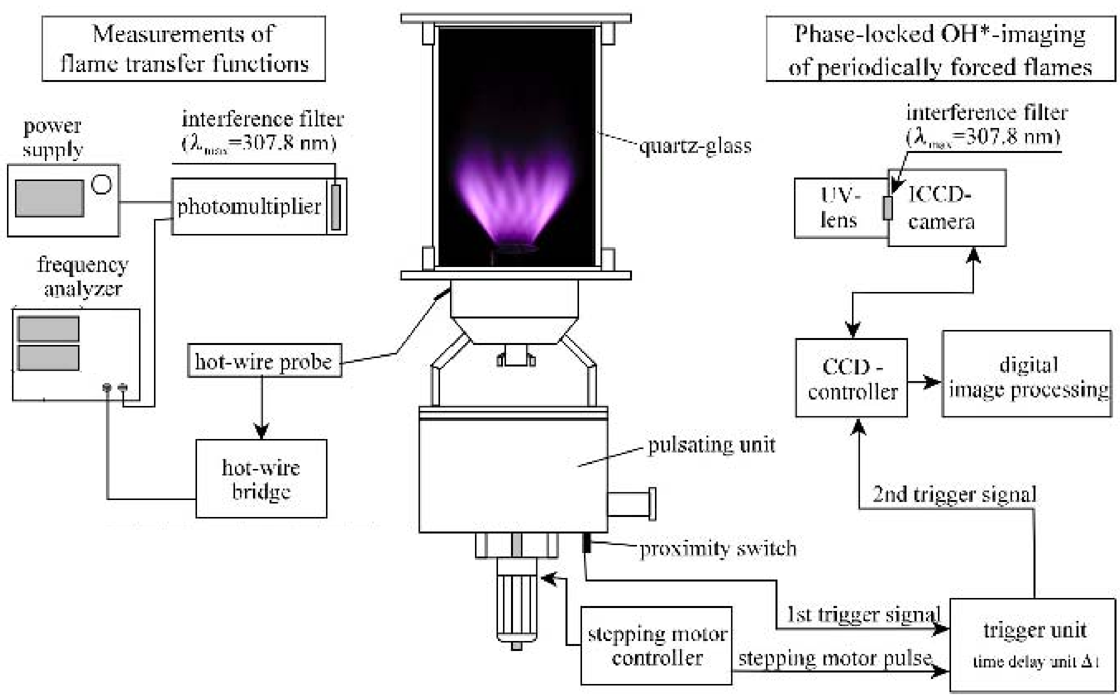

Figure 3: Experimental setup.

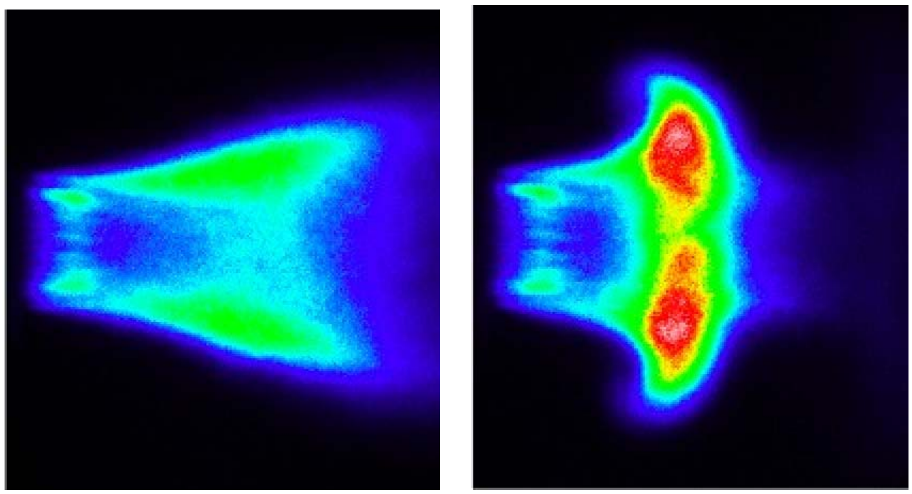

quasi-steady flame **ring vortices**

Figure 4: OH images of the flame structure.

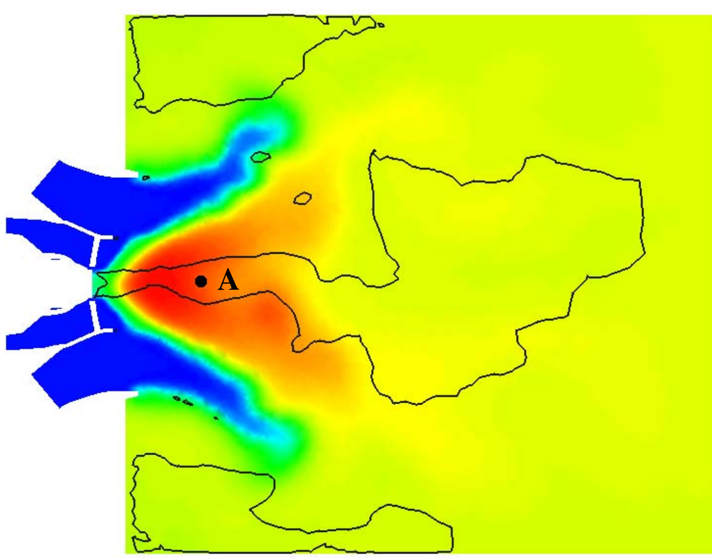

Figure 5: Field of temperature in the axial plane, ——— : zero axial velocity.

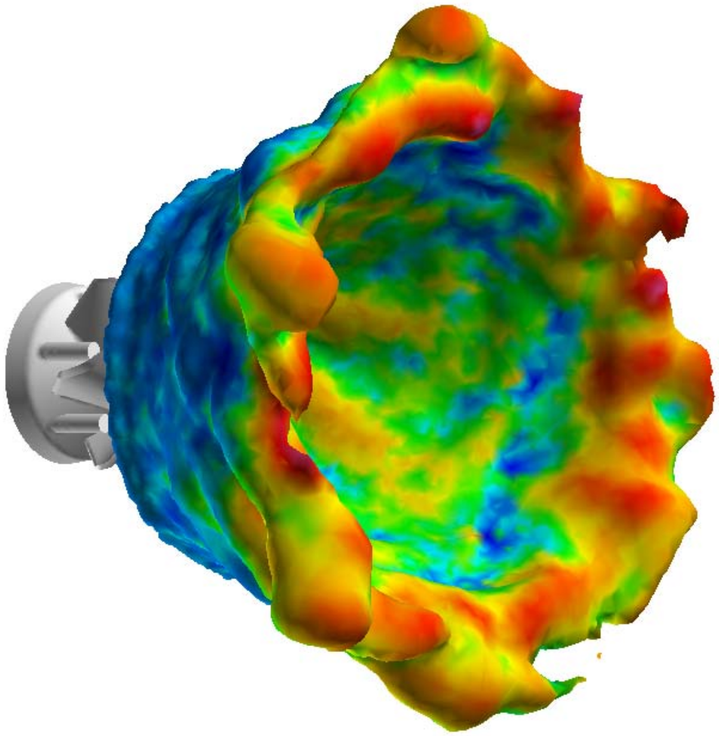

Figure 6: Snapshot of temperature iso-surface (1000 K) colored by axial velocity.

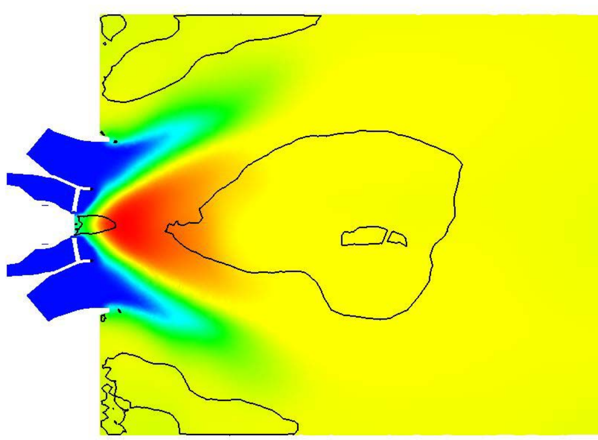

Figure 7: Longitudinal cut colored by average temperature, ——— : zero axial velocity.

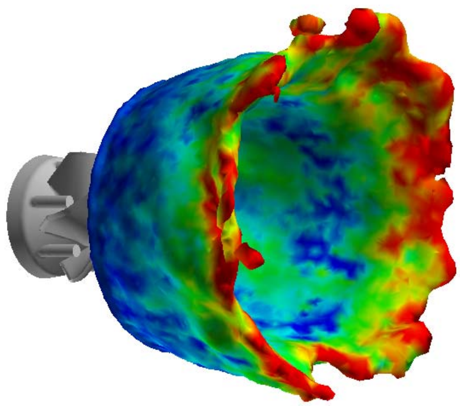

(a)

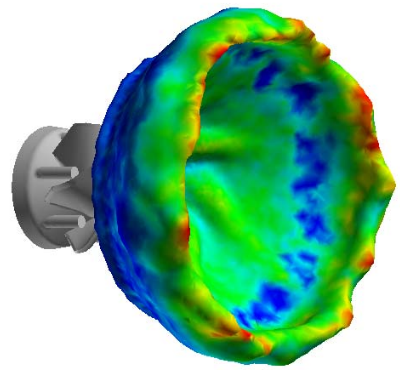

(b)

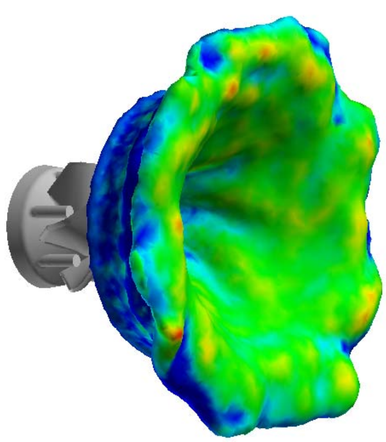

(c)

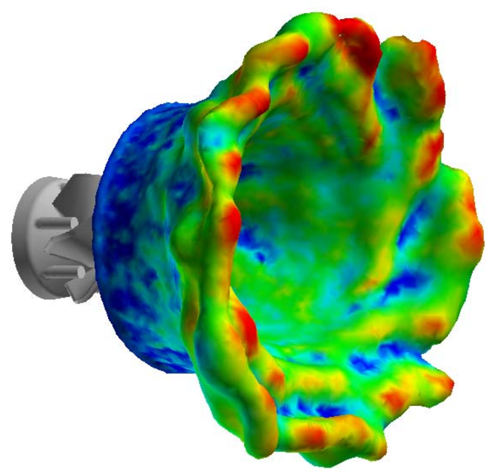

(d)

Figure 8: Snapshots of temperature iso-surface (1000 K) colored by axial velocity for four different phases of the pulsation cycle. (a) to (d) refer to Fig. 9.

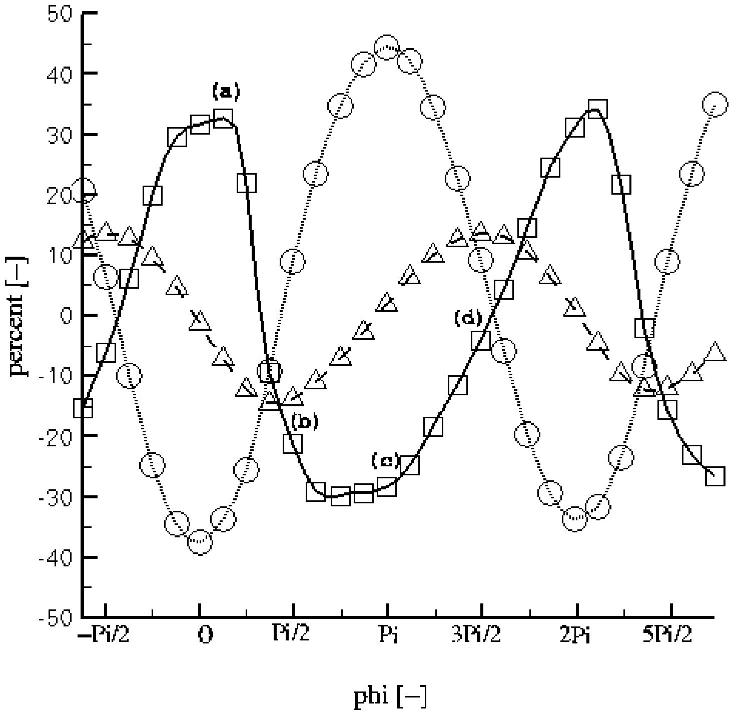

Figure 9: Heat release (squares), Inlet normal velocity (circles) and fuel mass (deltas) fluctuations in percents of mean values for the 120Hz LES simulation.

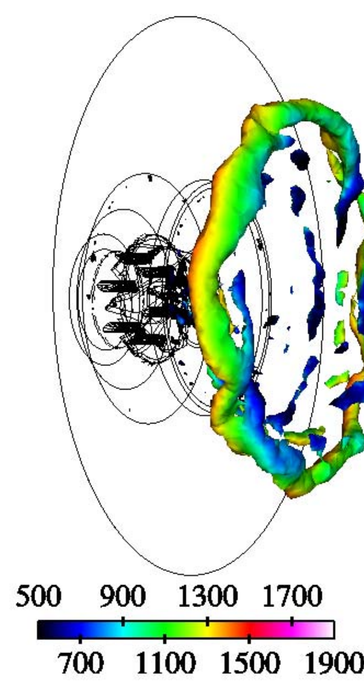

Figure 10: Isosurface of vortex criterion colored by temperature (Hussain[25]) visualising the vortex ring structure.

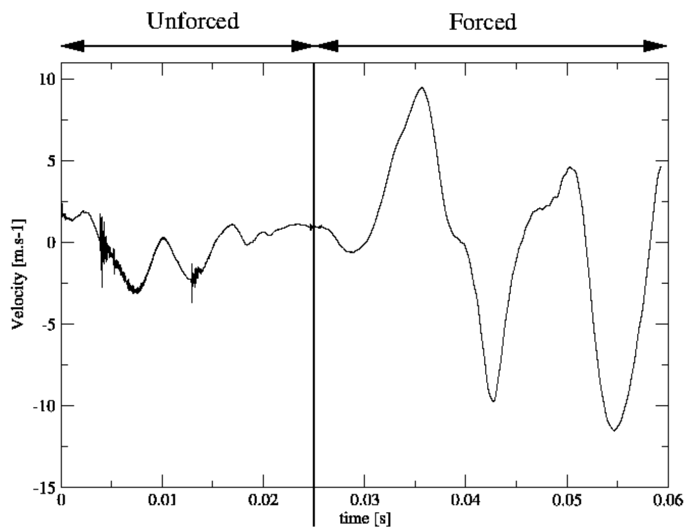

Figure 11: Radial velocity at point A (Fig. 5) for a 120 Hz pulsation.

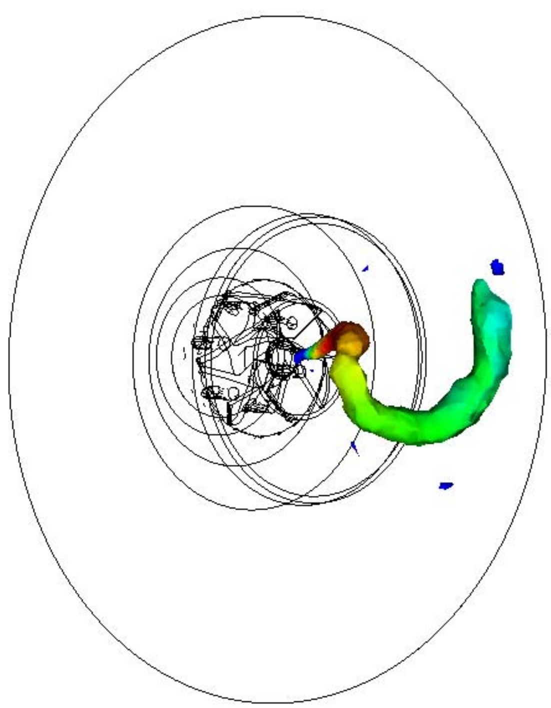

Figure 12: Isosurface of vortex criterion colored by temperature visualising the precessing vortex core.

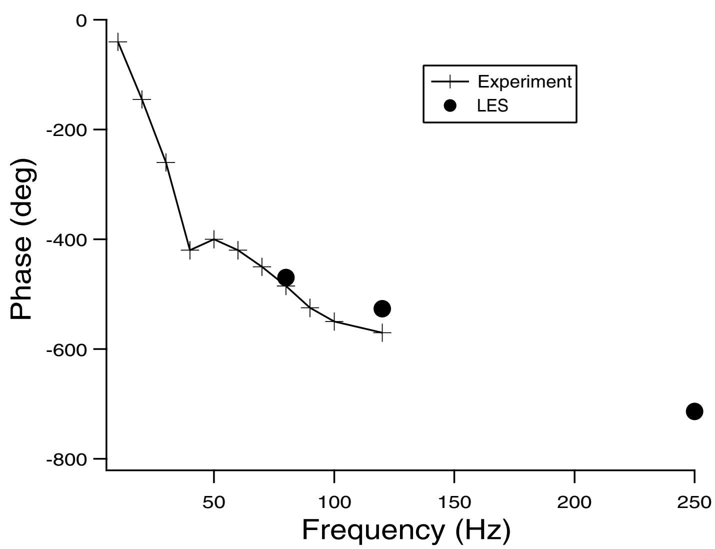

Figure 13: Comparison of LES and experiment time delay.